

1 *Type of the Paper (Article, Review, Communication, etc.)*

## 2 **A Deep Learning Approach for Wi-Fi based People 3 Localization**

4 **A. M. Khalili <sup>1,\*</sup>, Abdel-Hamid Soliman <sup>1</sup> and Md Asaduzzaman <sup>1</sup>**

5 <sup>1</sup> School of Creative Arts and Engineering, Staffordshire University, United Kingdom;

6 [a.soliman@staffs.ac.uk](mailto:a.soliman@staffs.ac.uk), [md.asaduzzaman@staffs.ac.uk](mailto:md.asaduzzaman@staffs.ac.uk)

7 \* Correspondence: [a.m.khalili@outlook.com](mailto:a.m.khalili@outlook.com)

8

9 **Abstract:** People localization is a key building block in many applications. In this paper, we propose  
10 a deep learning based approach that significantly improves the localization accuracy and reduces  
11 the runtime of Wi-Fi based localization systems. Three variants of the deep learning approach are  
12 proposed, a sub-task architecture, an end-to-end architecture, and an architecture that incorporates  
13 prior knowledge. The performance of the three architectures under different conditions is evaluated  
14 and the significant improvement of the three architectures over existing approaches is  
15 demonstrated.

16 **Keywords:** Deep learning; Compressive sensing; People localization; Signal detection; Wi-Fi.

17

---

### 18 **1. Introduction**

19 People localization is a key building block in many applications such as surveillance, activity  
20 classification, and elderly people monitoring. Video-based systems suffer from many limitations  
21 making them unable to operate in many real-world situations; for instance, they require users to be  
22 in the camera's line-of-sight, they can't work in the dark, through walls or smoke, and they violate  
23 users' privacy; furthermore, video-based tracking and localization algorithms suffer from low  
24 localization accuracy and high computational cost.

25 Wi-Fi provides an accessible source of opportunity for people localization, it doesn't have the  
26 limitations of video-based systems; furthermore, it has reasonable bandwidth and transmitted power.  
27 The potential to provide people localization by using this ubiquitous source of opportunity, and  
28 without transmitting any additional signal, nor requiring co-operation from the users, provides  
29 interesting opportunities. The users will be localized based on the available Wi-Fi signals that are  
30 reflected from their bodies.

31 Recently, a number of Wi-Fi based localization systems were proposed [1-3], and [7-10]. A multi-  
32 person localization system was proposed by Adib et al. [1], they determined users' locations based  
33 on the reflections of Wi-Fi signals from their bodies, the results show that their system was able to  
34 localize up to five people at the same time with an average accuracy of 11.7 cm. Colone et al. [2]  
35 studied the use of Wi-Fi signals for people localization, they have conducted an ambiguity function  
36 analysis for Wi-Fi signals. They have also studied the range resolution for both direct sequence spread  
37 spectrum (DSSS) and orthogonal frequency division multiplexing (OFDM) frames, for both the range  
38 and the Doppler dimensions, large sidelobes were detected, which explains the masking of closely  
39 spaced users. Chetty et al. [3] conducted an experiment in a high clutter indoor environment using  
40 Wi-Fi signals, they were able to detect one moving person behind a wall.

41 Compressive Sensing (CS) is a convenient approach to improve the accuracy and detect closely  
42 spaced users, which are difficult to separate using conventional methods. CS can also work at a lower  
43 rate than the Nyquist rate. The use of CS in radar has been recently investigated in [4, 5]. Anitori et  
44 al. [6] presented an architecture for adaptive CS radar detection with Constant False Alarm Rate  
45 (CFAR) properties, they also provided a methodology to predict the performance of the proposed  
46 detector. Researchers in [7] and [8] have shown that compressive sensing can detect objects with high  
47 accuracy using Wi-Fi signals.

48 Recently, there is a growing interest in using Deep Learning (DL) in communication and signal  
49 processing due to its ability in adapting to many imperfections that exist in real-world environments.  
50 DL has recently shown promising results in image recognition and classification [11-13]. The key  
51 factors behind these significant results are high-performance computing systems and the use of large  
52 amount of data such as the ImageNet dataset [14] which contains more than one million images.

53 In communication, researchers have recently used deep learning for modulation detection [15],  
54 channel encoding and decoding [16-21], and channel estimation [22-25]. Wang et al. [26] have recently  
55 surveyed the applications of DL in communication.

56 In [22], different deep learning architectures such as Deep Neural Network (DNN),  
57 Convolutional Neural Network (CNN), and Long Short-Term Memory (LSTM) were used for signal  
58 detection in a molecular communication system. Simulation results demonstrated that all these  
59 architectures were able to outperform the baseline, while the LSTM based detector has shown  
60 promising performance in the presence of Inter-Symbol Interference (ISI).

61 In [23], a deep learning based detector called DetNet was proposed, the aim was to reconstruct  
62 a transmitted signal  $x$  using the received signal  $y$ . To test the performance of the proposed approach  
63 in complex channel environments, two scenarios were considered, the fixed channel model and the  
64 varying channel model. DetNet was compared with two algorithms, the approximate message  
65 passing (AMP), and the semi-definite relaxation (SDR) which provide close to optimal detection  
66 accuracy. In the fixed channel scenario, the simulation results showed that DetNet was able to  
67 outperform AMP and achieves comparable accuracy to SDR but with a significant reduction of the  
68 computational cost (about 30 times faster). Similarly, in the varying channel scenario, DetNet was 30  
69 times faster than the SDR and showed a close accuracy.

70 In [24], a five layers fully connected DNN was used for channel estimation and detection of  
71 OFDM system by considering the channel as a black box. In the training phase, the data are passed  
72 through a channel model. The frequency domain signal representing the data information is then fed  
73 to the DNN detector that reconstructs the transmitted data. When comparing with the conventional  
74 minimum mean square error (MMSE) method, the DNN detector was able to achieve comparable  
75 performance. Then it was able to show better performance when fewer pilots are used, or when  
76 clipping distortion was introduced to decrease the peak-to-average power ratio.

77 In radar, Yonel et al. [27] have recently used deep learning for the inverse problem in radar  
78 imaging, they designed a recurrent neural network architecture and used it as an inverse solver. The  
79 results show that the proposed approach was able to outperform conventional methods in terms of  
80 the computation time and the reconstructed image quality.

81 Deep learning has been also recently used for compressive sensing [28-30]. Although

82 compressive sensing has revolutionized signal processing, the main challenge facing it, is the slow  
83 convergence of current reconstruction algorithms, which limits the applicability of CS systems. In  
84 [28] a new signal reconstruction framework called DeepInverse was introduced. DeepInverse uses a  
85 convolutional network to learn the inverse transformation from measurements to signals. The  
86 experiments indicated that DeepInverse was able to closely approximate the results produced by  
87 state of the art CS reconstruction algorithms; however, it is hundreds times faster in runtime. This  
88 significant improvement in the runtime requires computationally intensive off-line training.  
89 However, the training needs to be done only once.

90 Recently, there is a trend of using deep learning for Wi-Fi based localization systems [31-35],  
91 [54]. Fang and Lin [31] proposed a system that uses a neural network with a single hidden layer to  
92 extract features from Received Signal Strength (RSS). It was able to improve the localization error to  
93 below 2.5m, which is 17% improvement over state of the art approaches. A system called DeepFi was  
94 proposed in [33] with four layers neural network. DeepFi was able to improve the accuracy by 20%  
95 over the FIFS system, which uses a probability based model. A system called CiFi was proposed in  
96 [34], it used a convolutional network for indoor localization based on Wi-Fi signals. First, the phase  
97 data was extracted from the channel state information (CSI), then the phase data is used to estimate  
98 the angle of arrival (AOA), which is used as an input to the convolutional network. The results show  
99 that CiFi has an error of less than 1 m for 40% of the test locations, while for other approaches it is  
100 30%. In addition, it has an error of less than 3 m for 87% of the test locations, while for DeepFi it is  
101 73%. In [35], A system called ConFi was proposed, which is a CNN based Wi-Fi localization technique  
102 that uses CSI as features. The CSI was organized as a CSI feature image, where the CSIs at different  
103 times and different subcarriers were arranged into a matrix. The CNN consists of three convolutional  
104 layers and two fully connected layers. The network is trained using the CSI feature images. ConFi  
105 was able to reduce the mean error by 9.2% and 21.64% over DeepFi and DANN respectively.

106 These results show the significant improvement in the runtime and the accuracy of deep learning  
107 based systems. However, RSS provides only coarse-grained information about the wireless channel  
108 variations. CSI can capture fine-grained variations in the wireless channel. It also contains the  
109 amplitude and the phase measurements for each OFDM subcarrier. However, using the reflected  
110 signals from the bodies of the users can capture more valuable information such as the Doppler shift,  
111 therefore the latter approach will be used in this work.

112 In this paper, we investigate the use of deep learning for Wi-Fi based localization systems. The  
113 main contribution of this paper is a deep learning based Wi-Fi localization technique that significantly  
114 improves the accuracy and reduces the runtime in comparison with existing techniques. Three  
115 architectures are proposed, an end-to-end architecture, a sub-task architecture, and an architecture  
116 that introducing prior knowledge. The performance of the proposed approach is evaluated in the  
117 presence of multipath propagation. The role of each parameter of the training set and the effect of  
118 each parameter of the network are also investigated.

119 The paper is organized as follows: Section 2 describes the Wi-Fi signal model. An overview of  
120 compressive sensing is given in Section 3. An overview of deep learning is given in Section 4. Section  
121 5 introduces the detection method using the compressive sensing approach. The deep learning based  
122 localization technique is introduced in Section 6. Simulation results are listed in Section 7. Section 8

123 discusses the results and future research directions, and the paper is concluded in Section 9.

124 **2. Wi-Fi Signal Model**

125 Wi-Fi standards IEEE 802.11 [36] use both DSSS modulation in the 802.11b standard with 11MHz  
 126 bandwidth and OFDM with 20MHz bandwidth in the newer a/g/n standards. In OFDM, the signal is  
 127 divided into  $N_s$  symbols, then these symbols are modulated onto multiple subcarriers. The duration  
 128 of each OFDM symbol is  $T$ . The spacing of the subcarrier is  $\Delta f = 1/T$  and the bandwidth is  $B = N_s \Delta f$ .  $f_c$   
 129 is the carrier frequency, and  $f_m = f_c + m\Delta f$  is the frequency of the  $m$ th subcarrier. A cyclic prefix (CP)  
 130 is used to avoid inter-symbol interference,  $T_{cp}$  denotes the length of the CP. One OFDM symbol in the  
 131 baseband is given by

$$132 \quad x(t) = \sum_m s[m] e^{j2\pi m \Delta f t} q(t) \quad (1)$$

133

134 Where  $s[m]$  is the symbol of the  $m$ th subcarrier and  $q(t)$  is a rectangular window of length  $T_{cp} + T$ . We  
 135 consider a uniform linear array with  $N$  elements and  $P$  signals impinge on the array from directions  
 136  $\theta_1, \theta_2, \dots, \theta_P$ , respectively, the received Wi-Fi signals can be expressed by

137

$$138 \quad y(t) = \sum_p a(\theta_p) A_p e^{j2\pi f_{cap} t} x(t - \tau_p) + w(t) \quad (2)$$

139

140 Where  $w(t)$  is white Gaussian noise and  $A_p$  is the attenuation which includes the path loss and the  
 141 reflection,  $\tau_p$  is the delay and  $a_p$  is the range rate of the  $p$ th path divided by the speed of light,  $x(t)$  is  
 142 an OFDM symbol and the steering vector  $a(\theta_p)$  is expressed by

143

$$144 \quad a(\theta_p) = [e^{-j2\pi d \cos(\theta_p)/\lambda} \dots e^{-j2\pi L d \cos(\theta_p)/\lambda}] \quad (3)$$

145

146 Where  $\lambda$  is the signal wavelength,  $d$  is the array inter-element spacing and  $L$  is the number of  
 147 antennas.

148 **3. Compressive Sensing**

149 Consider a discrete-time signal  $x$  of length  $N$ .  $x$  can be represented in terms of basis vectors  $\psi_i$

$$150 \quad x = \sum_{i=0}^N s_i \psi_i \quad (4)$$

151 Where  $s_i$  is weighting coefficients. When  $x$  is a linear combination of a small number of  $K$  basis  
 152 vectors, with  $K < N$ , i.e., only  $K$  vectors of  $s_i$  in (4) are non-zero; then, compressive sensing allows to  
 153 sample  $x$  with a smaller number of measurements than the Nyquist rate. Measurements  $y$  with  $M <$   
 154  $N$  are performed by linear projections

$$155 \quad y = \Phi x + n \quad (5)$$

156 With a measurement matrix  $\Phi$  and additive noise  $n$ . When  $x$  is sparse with only a small number of  
 157 non-zero entries  $K < N$ , compressive sensing can reconstruct  $x$  given that the measurement matrix  $\Phi$   
 158 is incoherent with the basis  $\psi$ , i.e., the vectors  $\{\phi_i\}$  cannot sparsely represent the vectors  $\{\psi_i\}$ . The

159 compressive sensing reconstruction problem then can be formulated as a convex optimization  
160 problem

161 
$$\hat{x} = \min_{x^*} ||x^*||_1 \text{ subject to } ||y - \Phi x^*||_2 \leq \varepsilon \quad (6)$$

162 Where  $\varepsilon$  bounds the noise in the signal.

163 **4. Deep Learning**

164 Deep learning [37, 38] is inspired from neural systems in biology, where the weighted sum of many  
165 inputs is fed to an activation function such as the sigmoid function, to produce an output. The neural  
166 network is then built by linking many neurons to form a layered architecture. A loss function, such  
167 as the mean square error should be used to get the weights that minimize the loss function between  
168 the expected output and output of the network. Optimization algorithms such as the Gradient  
169 Descent (GD) are typically used in the training to find the best parameters. In [39] it has been shown  
170 that neural network can be used as a universal function approximator by introducing hidden layers  
171 between the output and the input layers.

172 In the fully connected feedforward neural network, each neuron is linked to the adjacent layers.  
173 Efficient algorithms such as the backpropagation were proposed for training such networks. Many  
174 problems could arise during the training process, such as converging to a local minimum. To address  
175 this problem, many adaptive learning algorithms such as the Adam algorithm were proposed.  
176 However, although the trained network can perform well using the training data, the network might  
177 perform very poorly using the testing data because of overfitting. Many techniques have been  
178 proposed to reduce overfitting such as dropout.

179 Recurrent Neural Network (RNN) was introduced to provide neural networks with memory,  
180 where in many situations, the outputs need also to depend on the input from previous time steps.  
181 One example is translation, where the knowledge of previous words in the sentence would  
182 significantly help in producing a better translation of the current word. Some recently used RNN  
183 architectures that are showing promising results include Gated Recurrent Unit (GRU), and LSTM.

184 The convolutional neural network is another promising architecture. The basic idea of the CNN  
185 is to use convolutional and pooling layers before the fully connected network. In the convolutional  
186 layer, a number of filters are learned to represent local spatial patterns along the input channels. The  
187 pooling layer performs down-sampling, where the number of parameters is significantly decreased  
188 before the fully connected layers.

189 With the promising results of the CNN architecture in computer vision, many researchers have  
190 attempted to improve the CNN architecture proposed by Krizhevsky et al. [11] to achieve better  
191 accuracy. For example, the highest accuracy architecture submitted to the ImageNet Large Scale  
192 Visual Recognition Competition (ILSVRC) in 2013 [12] used smaller stride and smaller window size  
193 for the convolutional layers. In [40], the researchers have addressed another important architecture  
194 design aspect, which is the network depth. Recent evidence [40, 41] shows that the network depth is  
195 of crucial importance. However, the main challenge of using deeper networks is the vanishing  
196 gradients problem [42, 43], which affects the convergence significantly. To address the vanishing  
197 gradient problem, new activation functions such as the Rectified Linear Units (ReLU) were

198 introduced instead of the sigmoid function. The problem was also addressed by introducing  
 199 normalized initialization [43, 44] and batch normalization layers [45], which were able to make  
 200 networks with tens of layers to begin converging. However, with the increased network depth, the  
 201 accuracy gets saturated and then rapidly degrades [46, 47]. In [46], the researchers have addressed  
 202 the degradation problem by proposing a deep residual learning approach. To maximize the  
 203 information flow, skip connections were introduced. The 152 layers residual network was applied on  
 204 the ImageNet dataset, it was able to win the first place in the ILSVRC 2015 competition. To ensure  
 205 maximum information flow between different layers of the network, all layers are connected to each  
 206 other directly in [49]. Where each layer connects its output to all subsequent layers and gets inputs  
 207 from all preceding layers.

208 **5. Wi-Fi based localization Using Compressive Sensing**

209 In this section, we describe a Wi-Fi localization method using compressive sensing, where the works  
 210 of [7] and [8] are extended to also include the angle of arrival estimation. The number of objects is  
 211 often very small compared to the number of points in the scene, this implies that the scene is sparse,  
 212 which enable us to formulate a CS reconstruction problem and solve it using convex optimization.  
 213 The received signal should be matched to delay-Doppler-angle combinations, corresponding to  
 214 objects detections. A sufficient delay-Doppler-angle resolution should be considered; however, a very  
 215 high resolution may lead to a large number of combinations, many of them are highly correlated. The  
 216 delay-Doppler-angle scene is divided into a  $P \times V \times Z$  matrix, in which each point represents a unique  
 217 delay-Doppler-angle point, the sparse vector  $x$  is composed of  $P$  data points in the range dimension  
 218 and  $Z$  data points in the angle dimension at all considered Doppler shifts with  $V$  data points in the  
 219 Doppler dimension. The size of vector  $x$  is  $Q = PVZ$ . The  $pvz$  index will be nonzero if an object exists  
 220 at the point  $(p, v, z)$ . The measurements vector  $y$  contains the data from  $L$  antennas at time  $t_i$ . The  
 221 measurement matrix  $\Phi$  is generated by creating time-shifted versions of the transmitted signal  
 222 (represented by (7)) for each Doppler frequency and each angle of arrival.

223 
$$F = [ s(t) \ s(t - \tau_1) \ \dots \ s(t - \tau_p) ] \quad (7)$$

224 We assume that  $s(t)$  is known. The measurement matrix  $\Phi$  establishes a linear relation between the  
 225 measurements at multiple antennas  $[y_1 \ y_2 \ \dots \ y_L]$  with the range profile  $[x_1 \ x_2 \ \dots \ x_Q]$  at different  
 226 Doppler shifts  $\omega_v$  and different angles  $\theta_z$ .

227

228 
$$\begin{bmatrix} y_1 \\ y_2 \\ \vdots \\ y_L \end{bmatrix} = \Phi \begin{bmatrix} x_1 \\ x_2 \\ \vdots \\ x_Q \end{bmatrix} \quad (8)$$

229 Where  $\Phi$  is expressed by

230

231 
$$\begin{pmatrix} e^{-\frac{j2\pi d\cos(\theta_1)}{\lambda}} e^{j\omega_1 t_1} F & \dots & e^{-\frac{j2\pi d\cos(\theta_z)}{\lambda}} e^{j\omega_1 t_1} F & \dots & e^{-\frac{j2\pi d\cos(\theta_1)}{\lambda}} e^{j\omega_v t_1} F \dots e^{-\frac{j2\pi d\cos(\theta_z)}{\lambda}} e^{j\omega_v t_1} F \\ e^{-\frac{j2\pi 2d\cos(\theta_1)}{\lambda}} e^{j\omega_1 t_1} F & \dots & e^{-\frac{j2\pi 2d\cos(\theta_z)}{\lambda}} e^{j\omega_1 t_1} F & \dots & e^{-\frac{j2\pi 2d\cos(\theta_1)}{\lambda}} e^{j\omega_v t_1} F \dots e^{-\frac{j2\pi 2d\cos(\theta_z)}{\lambda}} e^{j\omega_v t_1} F \\ \vdots & & \ddots & & \vdots \\ e^{-\frac{j2\pi Ld\cos(\theta_1)}{\lambda}} e^{j\omega_1 t_1} F & \dots & e^{-\frac{j2\pi Ld\cos(\theta_z)}{\lambda}} e^{j\omega_1 t_1} F & \dots & e^{-\frac{j2\pi Ld\cos(\theta_1)}{\lambda}} e^{j\omega_v t_1} F \dots e^{-\frac{j2\pi Ld\cos(\theta_z)}{\lambda}} e^{j\omega_v t_1} F \end{pmatrix}$$

232

233 To improve the detection probability, the results of 10 signals are combined before the threshold step,  
 234 where the final value of the object is equal to the count of its appearance across all the 10 reconstructed  
 235 scenes.

236 **6. Method**

237 Most signal processing techniques in communications and radar have solid foundations in  
 238 information theory and statistics, and are optimal using some assumptions such as linearity, and  
 239 Gaussian statistics. However, many imperfections exist in real-world environments. Deep learning is  
 240 a very appealing option because it can adapt to real-world imperfections, which can't be always  
 241 captured by analytical models.

242 Choosing the suitable architecture and its parameters, which best suit the problem is an  
 243 important question. We have tried many architectures with different number and size of layers, the  
 244 best performing architecture is shown in Table 1. The roles of different parameters of the proposed  
 245 architecture will be evaluated in the next section. The network has three convolutional layers and  
 246 three fully connected layers. The input of the network is the received signal  $y$ . Different kernels  
 247 (filters) can detect different features from the input signal and will construct different feature maps.  
 248 50 kernels and kernels of size 5 were found to work best in our model. For the fully connected layers,  
 249 the width of each layer is 800, and a 25% dropout is used to avoid overfitting. Dropout [48] means  
 250 temporarily removing units from the network with all their connections, the choice of which units to  
 251 remove is random. This will make each unit more robust and reduces its dependence on other units  
 252 to create useful features. To introduce non-linearity into the network, the ReLU is used as an  
 253 activation function. ReLU has shown higher performance than the sigmoid function and is more  
 254 plausible in biological systems. To accelerate the training process and to further reduce the  
 255 overfitting, batch normalization [45] is used in the proposed architecture. Vanishing gradients or  
 256 getting trapped in a local minimum may occur when using a high learning rate. However, by  
 257 normalizing the activations throughout the network, small changes are prevented from amplifying  
 258 to large changes in activations in gradients. Batch normalization has also shown promising results in  
 259 reducing overfitting. Softmax is used as an activation function in the output layer, softmax takes the  
 260 advantage that the locations are mutually exclusive, i.e. the object can be at one location only, softmax  
 261 will also output a probability for each location.

262

263 **Table 1.** The architecture of the network

Layer type	Parameters	Activation Function
Convolutional layer	Kernels number = 50 Kernel size = 5 Batch normalization	ReLU

Convolutional layer	Kernels number = 50 Kernel size = 5 Batch normalization	ReLU
Convolutional layer	Kernels number = 50 Kernel size = 5 Batch normalization	ReLU
Fully connected layer	800 neurons Batch normalization 25% dropout	ReLU
Fully connected layer	800 neurons Batch normalization 25% dropout	ReLU
Fully connected layer	800 neurons Batch normalization 25% dropout	ReLU
Fully connected layer	30 neurons	Softmax

264

265 The Adam optimizer is used to train the network and the training rate is set to 0.01. The used accuracy  
 266 metric is given by (9)

267

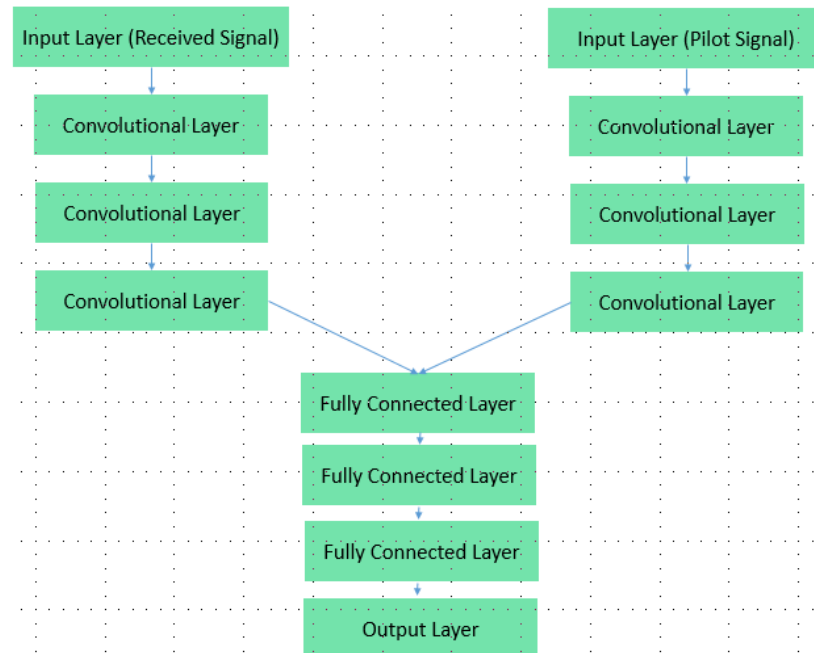
$$268 \quad Accuracy = \frac{TP}{P} \quad (9)$$

269

270 Where TP is the number of correct detections, and P is the number of positive cases. To be able to  
 271 compare the results of the deep learning approach with the compressive sensing approach, the same  
 272 accuracy metric will be also used to evaluate the performance of the compressive sensing approach.

273 Three variants of the above architecture will be used. The first one seeks to simplify the problem  
 274 and reduces its dimensionality by using several copies of the above network to estimate the location  
 275 of each user alone, where the first network will be trained to estimate the location of the first user,  
 276 the second network will be trained to estimate the location of the second user, and so on. The second  
 277 variant will use an end-to-end approach where the performance of the whole system can be  
 278 optimized. The above network will be used to estimate the locations of all users at the same time;  
 279 however, several output layers are added to estimate the locations of different users. The third variant  
 280 will introduce prior knowledge to the network by feeding the used pilot signal as an input to the  
 281 network, where the above network is modified by adding one more input layer for the used pilot  
 282 signal, followed by three convolutional layers, then the two branches are merged and the same fully  
 283 connected layers are used. Fig. 1 shows the modified architecture. The performance of these three  
 284 variants will be compared in the next section. Similar to the CS based approach, the output of the  
 285 network for 10 signals will be combined.

286



287

288 **Fig 1.** A DL architecture where prior knowledge is incorporated

289

290 The training data is obtained by simulation. In each simulation, an OFDM frame is formed. The  
 291 training data consists of 250000 examples, the input represents the received signal, which is described  
 292 in section 2, and the output represents the locations of the users in the scene, where the output will  
 293 be one at the user position and zero elsewhere. The training approach in [51] is used to train the  
 294 network by starting the training at high Signal to Noise Ratio (SNR) and then gradually reducing it.  
 295 The network is trained to minimize the difference between the output data and output of the neural  
 296 network. A test set will be used after the training to test the performance of the network, the size of  
 297 the test set is chosen to be 15% of the size of the training set. Since the network hasn't seen the test set  
 298 during the training phase, using the test set in calculating the accuracy would be a good  
 299 approximation of the generalization ability of the network.

300 **7. Results**

301 Computer simulations were performed to evaluate the proposed approach. We consider the 2.4GHz  
 302 industrial, scientific, and medical (ISM) band. The delay profile is represented by 30 samples, the  
 303 Doppler resolution is represented by 30 samples. The proposed approaches will be used to localize  
 304 users with random positions in the scene under different conditions. Training of the network took 12  
 305 hours on a standard Intel i3-4030U processor. First, we will compare the deep learning approach with  
 306 existing methods, then the performance of the proposed architectures will be compared. After that,  
 307 the performance of the deep learning approach is evaluated in the presence of multipath propagation.  
 308 Then, the role of each parameter of the training set is evaluated, and finally, the effect of each  
 309 parameter of the network is investigated.

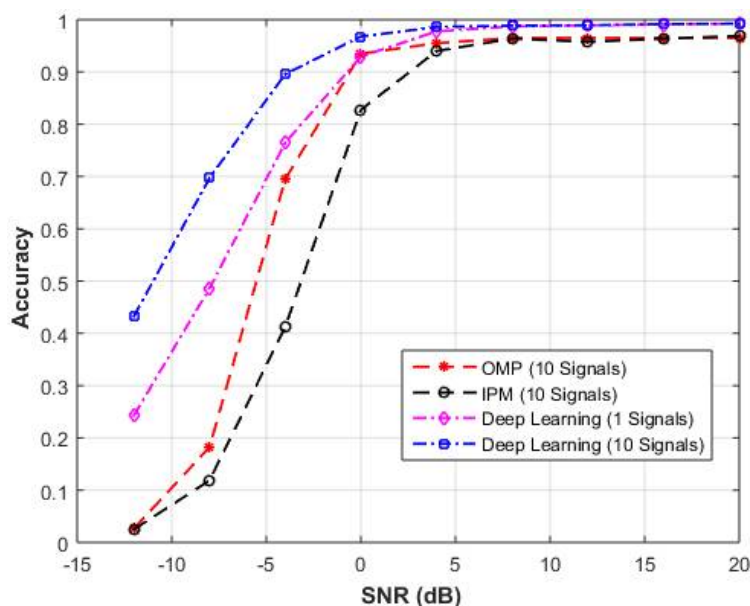
310

311 A. Comparison with other methods in terms of accuracy and runtime

312

313 To compare the proposed deep learning approach with the compressive sensing approach described  
 314 in section 5, 1000 Monte Carlo runs were performed to evaluate the compressive sensing approach  
 315 under different SNR values where the locations of the users are generated randomly. Both the  
 316 Orthogonal Matching Pursuit (OMP) [52] and the Interior Point Method (IPM) [53] were used to  
 317 reconstruct the scene. Each reconstructed scene is the result of combining 10 signals. The same  
 318 accuracy metric described in section 6 will be used to evaluate the CS approach. Fig. 2 shows the  
 319 percentage of correctly detecting four users for the OMP and the IPM versus the first DL architecture  
 320 which estimates the location of each object alone, the comparison is done for different SNR values,  
 321 and when a different number of signals is combined. The DL based approach is showing a significant  
 322 improvement in the accuracy, particularly for low SNR signals. This shows that the DL based  
 323 approach has a higher ability to adapt to noisy environments where the conventional approaches are  
 324 challenged.

325



326

327 **Fig 2.** The percentage of correctly detecting the persons for the OMP and the IPM versus the DL  
 328 approach for different SNR values and a different number of combined signals.

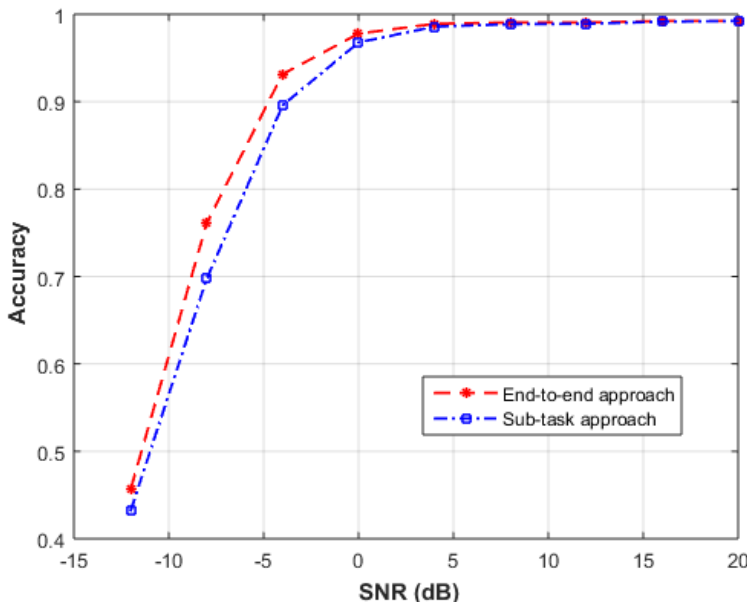
329

330 B. Comparing with an end-to-end approach

331

332 Two DL approaches will be compared, the first one tries to simplify the problem and reduces its  
 333 dimensionality by estimating the location of each user alone as described in section 6. The second  
 334 approach is an end-to-end approach where the locations of all users are estimated at the same time.  
 335 The end-to-end approach has shown a better performance, which suggests that the gain from  
 336 dividing this particular problem into simpler sub-tasks is lower than the gain from the overall  
 337 optimization of the whole problem. Fig. 3 shows the probability of correctly detecting the users under  
 338 different SNR values for the two approaches.

339



340

341 **Fig 3.** The probability of correctly detecting the users under different SNR values for the sub-task  
 342 approach and the end-to-end approach.

343

344 C. Comparing with an approach where prior knowledge is incorporating

345

346 Here we compare the end-to-end architecture with an architecture where prior knowledge is fed to  
 347 the network. The used pilot signal is also used as an input to the network to see whether it will  
 348 improve the performance of the network. The two approaches showed comparable results with a  
 349 very small improvement of the prior knowledge approach, which means that there is no much gain  
 350 from using additional information as an input to the network and the network is able to extract the  
 351 needed information from the received signal. Fig. 4 shows the probability of correctly detecting the  
 352 users under different SNR values for the two architectures.

353

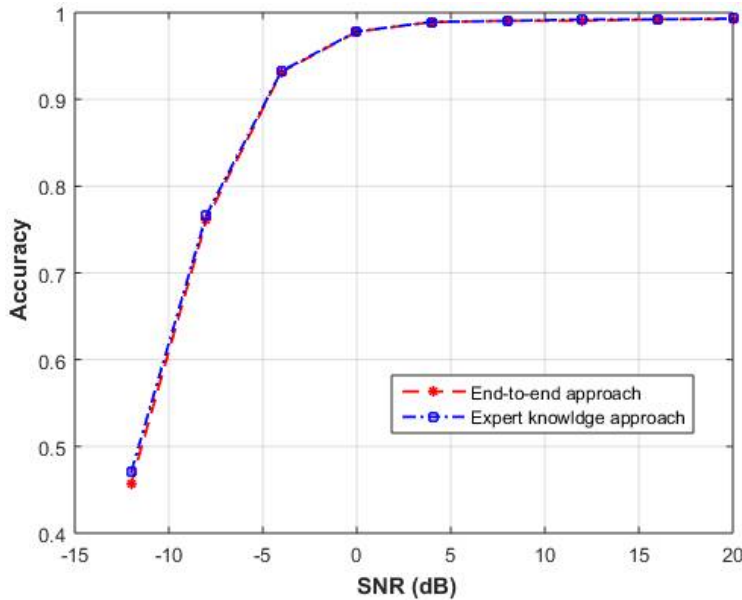
354 Table. 2 shows the runtime for the end-to-end approach versus the two CS approaches using a  
 355 standard Intel i3-4030U processor. The DL approach has significantly lower runtime than the CS  
 356 based approaches. Where, once the network is trained and the weights are calculated, predicting new  
 357 output involves relatively simple calculations.

358

**Table 2.** The runtime for the DL, the OMP, and the IPM methods.

Method	Runtime
DL	0.1803 seconds
OMP	0.4618 seconds
IPM	22.099 seconds

359



360

361 **Fig 4.** The probability of correctly detecting the users under different SNR values for the end-to-end  
 362 approach and the approach when prior knowledge is incorporated.

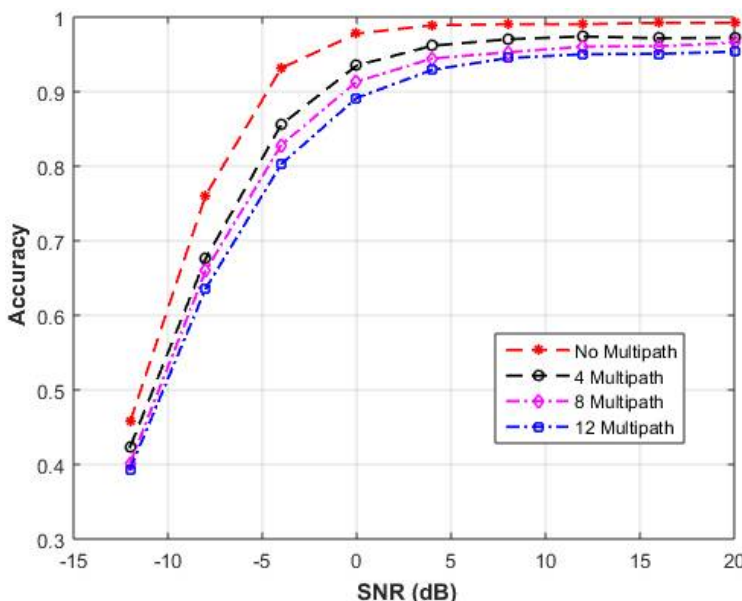
363

364 D. The effect of multipath

365

366 To investigate the effect of multipath signals, the proposed approach will be compared when 4, 8 and  
 367 12 multipath signals are added to the received signal. Fig. 5 shows that the end-to-end approach is  
 368 relatively robust to multipath propagation, where the network was able to cancel the multipath effect  
 369 and correctly detect the users.

370



371

372 **Fig 5.** The probability of correctly detecting the users under different SNR values when 4, 8 and 12  
 373 multipath signals are used.

374

375

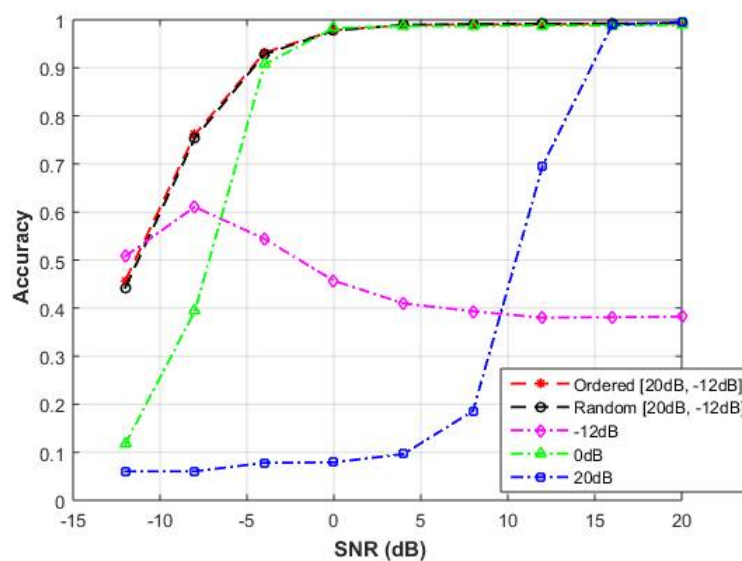
376

377 E. The effect of the SNR of the training set

378

379 To compare the effect of the SNR of the training samples, five sets will be tested. The first one contains  
380 signals with 20dB SNR, the second one contains signals with 0dB SNR, the third one contains signals  
381 with -12dB SNR, the fourth one contains signals with varying SNR starting from high SNR values to  
382 low SNR values i.e. from 20dB to -12dB, and the final set contains signals with varying SNR, however  
383 the signals here are sorted randomly. Fig. 6 shows the probability of correctly detecting the users  
384 under different SNR values for the five sets. Using the fourth and the fifth set have resulted in higher  
385 accuracy than the other sets, which means that the network should see examples from different SNR  
386 values. The -12dB set has shown higher accuracy at -12dB since there are more training samples at  
387 this SNR, however; the accuracy is much lower for other SNR values.

388



389

390 Fig 6. The probability of correctly detecting the users using training sets with different SNR values.

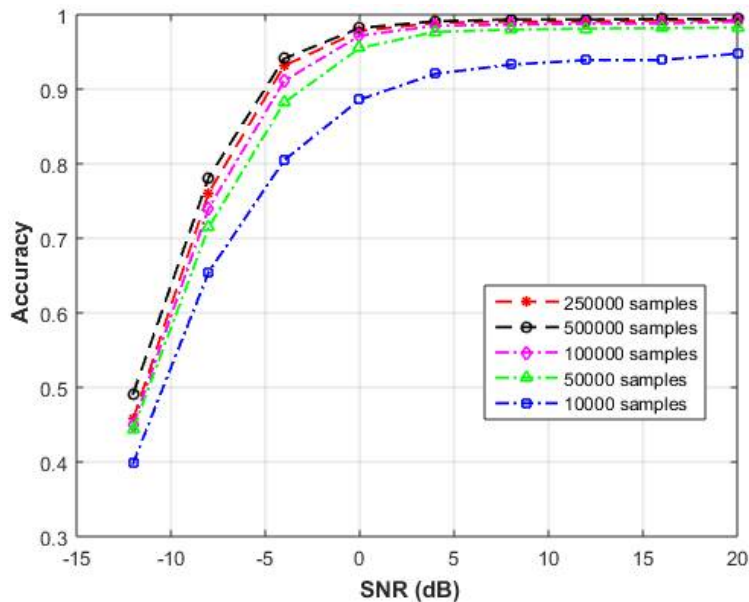
391

392 F. The effect of the number of examples

393

394 To investigate the effect of the number of the training examples on the performance of the proposed  
395 network, five sets with 10000, 50000, 100000, 250000, and 500000 training examples are compared.  
396 Fig. 7 shows the probability of correctly detecting the users under different SNR values for the five  
397 sets, the results show that the accuracy increases when a higher number of examples is used;  
398 however, the improvement becomes very small after 250000.

399



400

401 **Fig 7.** The probability of correctly detecting the users under different SNR values when different sizes  
402 of the training set are used.

403

404 G. The effect of different parameters of the network

405

406 Here we analyze the effect of different parameters on the performance of the network. First, we  
407 compare using a different number of neurons, then we compare using different number and sizes of  
408 kernels, and finally, we compare the role of dropout.

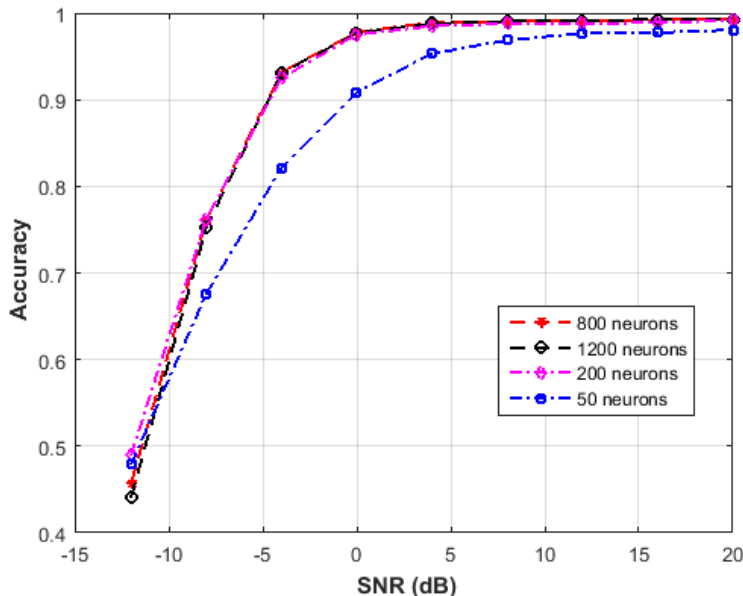
409

410 1. The effect of the number of neurons in each layer

411

412 Here we compare using a different number of neurons in each layer. 80, 200, 800, 1200 neurons are  
413 compared. Fig. 8 shows the probability of correctly detecting the users under different SNR values  
414 for the four cases. Increasing the number of neurons increases the accuracy; however, the difference  
415 between 200, 800 and 1200 is very small.

416



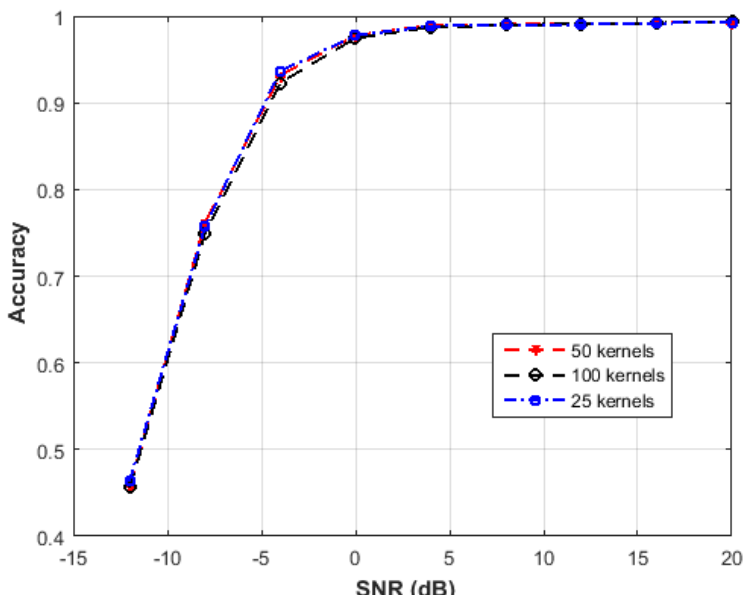
417

418 **Fig 8.** The probability of correctly detecting the users under different SNR values when a different  
 419 number of neurons is used.

420

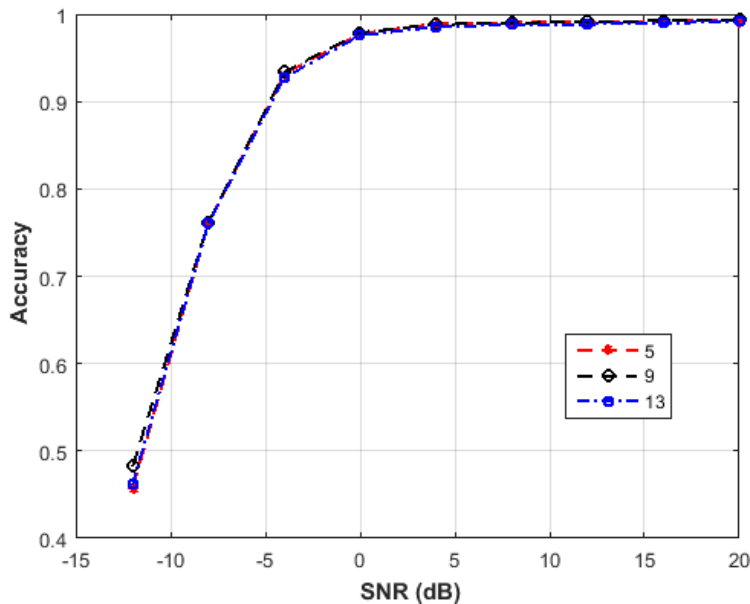
421 Then we compare changing the number of the kernels in the convolutional layers. 25, 50, and 100  
 422 kernels are compared. Fig. 9 shows the probability of correctly detecting the users under different  
 423 SNR values for the three cases. Increasing the number of kernels has not resulted in increasing the  
 424 accuracy where the three cases have shown comparable results.. Fig. 10 shows the results for different  
 425 sizes of the kernels, where kernels of size 9 are found to be slightly better in capturing useful features  
 426 from the signal.

427



428

429 **Fig 9.** The probability of correctly detecting the users under different SNR values when a different  
 430 number of kernels is used.



431

432 **Fig 10.** The probability of correctly detecting the users under different SNR values when different  
 433 sizes of the kernels are used.

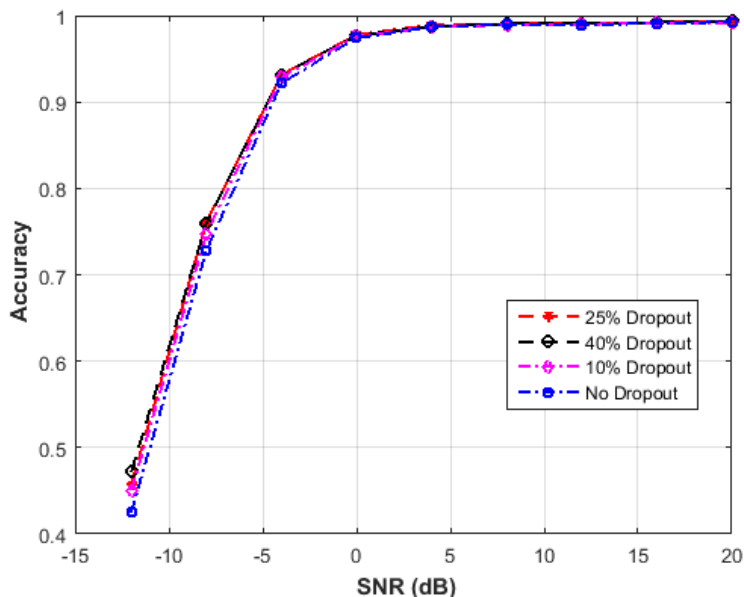
434

435 2. The effect of dropout

436

437 Here we compare the performance of the network for four cases, the first one is with no dropout, the  
 438 second one is with 10% dropout, the third one is with 25% dropout, and the fourth one is with 40%  
 439 dropout. Fig. 11 shows that increasing the dropout has resulted in more ability of the network to  
 440 create useful features where 25% and 40% dropout are showing slightly higher accuracy.

441



442

443 **Fig 11.** The probability of correctly detecting the users under different SNR values when different  
 444 percentages of dropout are used.

445

446

447 **8. Discussion**

448 The proposed deep learning approach has shown higher performance with less runtime in  
449 comparison with the CS approach. The proposed approach has also shown a high ability to adapt to  
450 challenging environments. For the studied problem, using deep learning for each sub-task and  
451 hence reducing the curse of dimensionality has resulted in less accurate results in comparisons with  
452 the end-to-end approach where the performance of the whole system is optimized. Introducing  
453 prior knowledge by using the pilot signal as an input to the network has not resulted in much  
454 improvement in the accuracy, where the network seems to be able to extract the needed  
455 information from the received signal. The proposed approach has also shown that it is relatively  
456 robust in multipath environments.

457 Increasing the number of examples in the training stage has resulted in higher accuracy;  
458 however, the improvement was very small after 250000. Using training examples from different  
459 SNR values has resulted in more accurate results in comparison of using the same SNR value for all  
460 the examples, whether that SNR is low or high. The results have also shown the role of different  
461 network parameters in improving the accuracy.

462 This work along with many other recent works have shown that deep learning has many  
463 potential applications in future signal processing, communication, and radar systems where  
464 conventional approaches are challenged. It represents a promising research direction that is still in  
465 its early stage. Some challenges still worth further investigations. Further research must be  
466 conducted to propose deep learning architectures that best suit signal processing, communication,  
467 and radar systems.

468 **9. Conclusions**

469 This paper has presented a Wi-Fi based localization technique based on deep learning, where  
470 three different architectures were proposed. Simulation results demonstrated the significant  
471 improvement in the accuracy and in the runtime of the proposed approaches over existing  
472 approaches. The end-to-end architecture was found to be more accurate than the other two  
473 architectures. The proposed approach has also shown that it is relatively robust in multipath  
474 environments. Future work will investigate further improvement in the localization accuracy by  
475 building architectures that best suit localization systems.

476

477 **Funding**

478 This research received no external funding

479 **Conflicts of Interest:**

480 The authors declare no conflict of interest.

481

482 **References**

- 483 1. Adib, F.; Kabelac, Z.; Katabi, D. Multi-person localization via RF body reflections. In Proceedings of  
484 the 12th USENIX Conference on Networked Systems Design and Implementation, Oakland USA, pp.  
485 279-292, May 2015.
- 486 2. Colone, F.; Woodbridge, K.; Guo, H.; Mason, D.; Baker, C.J. Ambiguity function analysis of wireless  
487 LAN transmissions for passive radar. IEEE Trans. Aerosp. Electron. Syst., 2011, vol. 47, no. 1, pp. 240-  
488 264.
- 489 3. Chetty, K.; Smith, G.; Guo, H.; Woodbridge, K. Target detection in high clutter using passive bistatic  
490 WiFi radar. Proc. IEEE Radar Conf, Pasadena, CA, USA, pp. 1-5, May 2009.

491 4. Ender, J. A brief review of compressive sensing applied to radar. IEEE 14th international radar  
492 symposium, pp. 3-16, June 2013.

493 5. Hadi, MA.; Alshebeili, S.; Jamil, K.; El-Samie, FE. Compressive sensing applied to radar systems: an  
494 overview. *Signal, Image and Video Processing*, 2015, vol. 9, no. 1, pp. 25-39.

495 6. Anitori, L.; Maleki, A.; Otten, M.; Baraniuk, RG.; Hoogeboom, P. Design and analysis of compressed  
496 sensing radar detectors. *IEEE Transactions on Signal Processing*, 2013, vol. 61, no. 4, pp. 813-27.

497 7. Maechler, P.; Felber, N.; Kaeslin, H. Compressive sensing for wifi-based passive bistatic radar. *Proc.*  
498 *20th IEEE European Signal Processing Conf*, Bucharest, Romania, pp. 1444-1448, August 2012.

499 8. Berger, C.R.; Zhou, S.; Willett, P. Signal Extraction Using Compressed Sensing for Passive Radar with  
500 OFDM Signals. *IEEE Int. Conf. Inf. Fusion*, pp. 1-6, July 2008.

501 9. Khalili, A.; Soliman, A. A. Track before mitigate: aspect dependence-based tracking method for  
502 multipath mitigation. *Electronics Letters*, 2016, vol. 52, no. 4, pp. 316-317.

503 10. Khalili, A.; Soliman, A. A.; Asaduzzaman, M. Quantum particle filter: a multiple mode method for low  
504 delay abrupt pedestrian motion tracking. *Electronics Letters*, 2015, vol. 51, no. 16, pp. 1251-1253.

505 11. Krizhevsky, A.; Sutskever, I.; Hinton, G. Imagenet classification with deep convolutional neural  
506 networks. In *NIPS*, 2012.

507 12. Zeiler, M. D.; Fergus, R. Visualizing and understanding convolutional neural networks. In *ECCV*, 2014.

508 13. Sermanet, P.; Eigen, D.; Zhang, X.; Mathieu, M.; Fergus, R.; LeCun, Y. Overfeat: Integrated recognition,  
509 localization and detection using convolutional networks. In *ICLR*, 2014.

510 14. Deng, J.; Dong, W.; Socher, R.; Li, L.J.; Li, K.; Fei-Fei, L. Imagenet: A large-scale hierarchical image  
511 database. In *Proc. CVPR*, 2009.

512 15. O'Shea, T. J.; Hoydis, J. An introduction to deep learning for the physical layer. *arXiv preprint*  
513 *arXiv:1702.00832*, 2017.

514 16. Nachmani, E.; Be'ery, Y.; Burshtein, D. Learning to decode linear codes using deep learning. in *Proc.*  
515 *Communication, Control, and Computing*, pp. 341-346, 2016.

516 17. Nachmani, E.; Marciano, E.; Burshtein, D.; Be'ery, Y. RNN decoding of linear block codes. *arXiv*  
517 *preprint arXiv:1702.07560*, 2017.

518 18. Gruber, T.; Cammerer, S.; Hoydis, J.; Brink, S. On deep learning-based channel decoding. in *Proc. of*  
519 *CISS*, pp. 1-6, 2017.

520 19. Gruber, T.; Cammerer, S.; Hoydis, J.; Brink, S. Scaling deep learning-based decoding of polar codes via  
521 partitioning. *arXiv preprint arXiv:1702.06901*, 2017.

522 20. Nachmani, E.; Marciano, E.; Lugosch, L.; Gross, W. J.; Burshtein, D.; Beery, Y. Deep learning methods  
523 for improved decoding of linear codes. *arXiv preprint arXiv:1706.07043*, 2017.

524 21. Liang, F.; Shen, C.; Wu, F. An iterative BP-CNN architecture for channel decoding. *arXiv preprint*  
525 *arXiv:1707.05697*, 2017.

526 22. Farsad, N.; Goldsmith, A. Detection algorithms for communication systems using deep learning.  
527 *arXiv preprint arXiv:1705.08044*, 2017.

528 23. Samuel, N.; Diskin, T.; Wiesel, A. Deep MIMO detection. *arXiv preprint arXiv:1706.01151*, 2017.

529 24. Ye, H.; Li, G. Y.; Juang, B.F. Power of deep learning for channel estimation and signal detection in  
530 OFDM systems. *arXiv preprint arXiv:1708.08514*, 2017.

531 25. Neumann, D.; Wiese, T.; Utschick, W. Learning the MMSE channel estimator. *arXiv preprint*  
532 *arXiv:1707.05674*, 2017.

533 26. Wang, T.; Wen, C. K.; Wang, H.; Gao, F.; Jiang, T.; Jin, S. Deep learning for wireless physical layer:  
534 Opportunities and challenges. *China Communications*, 2017, vol. 14, no. 11, pp. 92-111.

535 27. Yonel, B.; Mason, E.; Yazici, B. Deep Learning for Passive Synthetic Aperture Radar. *IEEE Journal of*  
536 *Selected Topics in Signal Processing*, 2018, vol. 12, no. 1, pp. 90-103.

537 28. Mousavi, A.; Baraniuk, R. G. Baraniuk, Learning to invert: Signal recovery via deep convolutional  
538 networks. In *Acoustics, Speech and Signal Processing (ICASSP)*, IEEE International Conference on, pp.  
539 2272-2276, March 2017.

540 29. Mousavi, A.; Patel, A. B.; Baraniuk, R. G. A deep learning approach to structured signal recovery. in  
541 *Proc. Allerton Conf. Communication, Control, and Computing. IEEE*, pp. 1336-1343, 2015.

542 30. Kulkarni, K.; Lohit, S.; Turaga, P.; Kerviche, R.; Ashok, A. Reconnet: Non-iterative reconstruction of  
543 images from compressively sensed random measurements. *Proc. IEEE Int. Conf. Comp. Vision, and*  
544 *Pattern Recognition*, 2016.

545 31. Fang S. H.; Lin, T. N. "Indoor location system based on discriminant adaptive neural network in IEEE  
546 802.11 environments," *IEEE Trans. Neural Network*, 2008, vol. 19, no. 11, pp. 1973–1978.

547 32. Wang, X.; Gao, L.; Mao, S. CSI phase fingerprinting for indoor localization with a deep learning  
548 approach. *IEEE Internet Things J*, 2016, vol. 3, no. 6, pp. 1113–1123.

549 33. Wang, X.; Gao, L.; Mao, S.; Pandey, S. CSI-based fingerprinting for indoor localization: A deep learning  
550 approach. *IEEE Trans. Veh. Technol*, 2017, vol. 66, no. 1, pp. 763–776.

551 34. Wang, X.; Wang, X.; Mao, S. Cifi: Deep convolutional neural networks for indoor localization with 5  
552 GHZ Wi-Fi. In *Communications (ICC), 2017 IEEE International Conference on*, pp. 1-6, May 2017.

553 35. Chen, H.; Zhang, Y.; Li, W.; Tao, X.; Zhang, P. ConFi: Convolutional Neural Networks Based Indoor  
554 Wi-Fi Localization Using Channel State Information. *IEEE Access*, 2017, vol. 5, pp. 18066-18074.

555 36. IEEE standard for information technology, part 11: Wireless LAN medium access control (mac) and  
556 physical layer (phy) specifications. June 2007.

557 37. Lecun, Y.; Bengio, Y.; Hinton, G. Deep learning. *Nature*, vol. 521, no. 7553, 2015.

558 38. Goodfellow, I.; Bengio, Y.; Courville, A. Deep learning. MIT press, 2016.

559 39. Hornik, K.; Stinchcombe, M.; White, H. Multilayer feedforward networks are universal approximators.  
560 *Neural networks*, 1989, vol. 2, no. 5, pp. 359–366.

561 40. Simonyan, K.; Zisserman, A. Very deep convolutional networks for large-scale image recognition. In  
562 *ICLR*, 2015.

563 41. Szegedy, C.; Liu, W.; Jia, Y.; Sermanet, P.; Reed, S.; Anguelov, D.; Erhan, D.; Vanhoucke, V.;  
564 Rabinovich, A. Going deeper with convolutions. In *CVPR*, 2015.

565 42. Bengio, Y.; Simard, P.; Frasconi, P. Learning long-term dependencies with gradient descent is difficult.  
566 *IEEE Transactions on Neural Networks*, 1994, vol. 5, no 2, pp. 157–166.

567 43. Glorot X.; Bengio, Y. Understanding the difficulty of training deep feedforward neural networks. In  
568 *AISTATS*, 2010.

569 44. He, K.; Zhang, X.; Ren, S.; Sun, J. Delving deep into rectifiers: Surpassing human-level performance on  
570 Imagenet classification. In *ICCV*, 2015.

571 45. Ioffe, S.; Szegedy, C. Batch normalization: Accelerating deep network training by reducing internal  
572 covariate shift. In *ICML*, 2015.

573 46. He, K.; and Sun, J. Convolutional neural networks at constrained time cost. In *CVPR*, 2015.

574 47. Srivastava, R. K.; Greff, K.; Schmidhuber, J. Highway networks. *arXiv:1505.00387*, 2015.

575 48. He, K.; Zhang, X.; Ren, S.; Sun, J. "Deep residual learning for image recognition," In *Proceedings of the*  
576 *IEEE conference on computer vision and pattern recognition*, pp. 770-778, 2016.

577 49. Huang, G.; Liu, Z.; Weinberger, K. Q.; van der Maaten, L. Densely connected convolutional networks.  
578 In *Proceedings of the IEEE conference on computer vision and pattern recognition*, p. 3, July 2017.

579 50. Srivastava, N.; Hinton, G.; Krizhevsky, A.; Sutskever, I.; Salakhutdinov, R. Dropout: A simple way to  
580 prevent neural networks from overfitting. *The Journal of Machine Learning Research*, vol. 15, no. 1,  
581 pp. 1929-1958.

582 51. George, D.; Huerta, E. Deep neural networks to enable real-time multimessenger astrophysics. *arXiv*  
583 preprint *arXiv:1701.00008*, 2016.

584 52. Tropp, J. A.; Gilbert, A. C. Signal Recovery from Random Measurements via Orthogonal Matching  
585 Pursuit. *IEEE Trans. Inf. Theory*, 2007, vol. 53, no. 12, pp. 4655 – 4666.

586 53. Dantzig, G.B.; Thapa, M.N. *Linear Programming 2: Theory and Extensions*. Springer-Verlag, 2003.

587 54. Jiang, H.; Cai, C.; Ma, X.; Yang, Y.; Liu, J. Smart Home based on WiFi Sensing: A Survey. *IEEE Access*,  
588 2018.